JOURNAL OF APPLIED POLYMER SCIENCE VOL. 19, PP. 179–198 (1975)

Reverse Osmosis Separation of Inorganic Solutes in Aqueous Solutions Using Porous Cellulose Acetate Membranes

TAKESHI MATSUURA, LUCIEN PAGEAU, AND S. SOURIRAJAN,
Division of Chemistry, National Research Council of Canada, Ottawa, Canada, K1A OR9

Synopsis

Using a modified form of the Born expression for the free energy of ion–solvent interaction, to both the bulk solution phase and the membrane–solution interface, a parameter is obtained to express the repulsion of the ion at the interface. This parameter, called the free energy parameter for ions, is then related to solute transport parameter obtained from reverse osmosis experiments. Numerical values of this free energy parameter have been obtained for six monovalent and four divalent cations and for 12 monovalent anions. Using the experimental data for the reverse osmosis separation of sodium chloride as reference, the utility of the above parameter for predicting solute separation in reverse osmosis is illustrated for 32 other inorganic salts.

INTRODUCTION

The physicochemical basis for reverse osmosis separation of inorganic ions in aqueous solutions using Loeb-Sourirajan-type porous cellulose acetate membranes has been discussed in the literature from several points of view. According to Lonsdale and co-workers,[1] reverse osmosis separation is governed by the solution–diffusion mechanism which requires solute and solvent dissolve in the membrane material and permeate through the membrane by diffusion through the homogeneous nonporous surface layer. Anderson and Heyde[2] have proposed a mechanism based on experimental partition coefficients of ionic solutes between water and cellulose acetate membrane material. According to Eisenman,[3–5] the selectivity of membranes for different ions depend on the relative free energy of interaction of ions between water and membrane material. McCutchan and co-workers[6,7] have tried to apply this approach to explain their data on reverse osmosis separations. Choi and Bennion[8] studied the membrane potential and relative mobilities of alkali and alkaline earth metal chlorides. They found that the relative mobilities were in the order

$$Li^+ < Na^+ < K^+ \gtrsim Rb^+ > Cs^+$$

and

$$Be^{++} > Mg^{++} < Ca^{++} < Sr^{++} > Ba^{++}$$

They reported that the hydrated radius appeared to control transport rate for small ions and crystallographic radius appeared to control transport rates for larger ions.

The analyses of Dytnerskii and co-workers,[9] Glueckauf,[10,11] and Bean[12] explicitly recognize that the surface layer (skin) of the membrane is microporous and heterogeneous. In the capillary filtration mechanism of Dytnerskii et al.,[9] the relative strength of the hydration envelope of ions governs solute separation and liquid permeation rate for a given membrane; with reference to anions, a measure of the strength of the ion hydrate envelope is given by the parameter $[Z_A^2/r_A - 0.25]$, where Z_A and r_A represent the valency and radius of the anion, respectively. In the analysis of Glueckauf[10,11] and Bean,[12] solute separation in reverse osmosis is governed by the electrostatic repulsion which ions experience in the vicinity of materials of low dielectric constant. Glueckauf's equation[10] predicts that solute separation increases with decrease in average pore size on the membrane surface, with decrease in ionic radius, with decrease in solute concentration in feed solution, with decrease in the dielectric constant of the membrane material, and/or with increase in the valency of the ion. Bean's equations[12] confirm the above predictions of the Glueckauf equation.

This work is in continuation of the investigations[13a,14] based on the preferential sorption–capillary flow mechanism according to which reverse osmosis separation is governed by two factors: (i) the relative magnitude of net repulsion of the solute molecules at the membrane–solution interface and (ii) the porous structure of the membrane surface. The repulsion of solute at the membrane–solution interface (i.e., negative adsorption of solute at the membrane–solution interface) is the net result of electrostatic and other interactions involving simultaneously the ion, solvent, and membrane material. Applying a modified form of the Born expression[15,16] for the free energy of ion–solvent interaction to both the bulk solution phase and the membrane–solution interface, a parameter is obtained to express the repulsion of the ion at the interface. This parameter, called the free energy parameter for ions, is then related to solute transport parameter in a manner similar to that reported earlier for alcohol solutes.[17] Using the experimental data involving 33 different inorganic salts in very dilute binary aqueous solutions, the numerical value of the ionic parameter for each of the six monovalent and four divalent cations and for the 12 monovalent anions has been calculated. The utility of the above free energy parameter for predicting solute separation in reverse osmosis is then illustrated.

EXPERIMENTAL

Thirty-three inorganic solutes listed in Table I (along with some relevant physicochemical data) were used in this work in single solute aqueous solutions. The apparatus and experimental procedure used were the same as those reported earlier.[14] Batch 316 (10/30)-type cellulose acetate mem-

TABLE I
List of Solutes Used with Some Physicochemical Data

Solute No.	Solute	λ_+^0 (ref. 29)	λ_-^0 (ref. 29)	$D_{AB} \times 10^5$, cm²/sec	$D_{AB} \times 10^5$, cm²/sec (ref. 13c)	$k \times 10^4$, cm/sec
1	LiF	38.66	55.4[a]	1.2127		13.3
2	LiCl	38.66	76.35	1.3667	1.366	14.4
3	LiBr	38.66	78.2	1.3777		14.5
4	$LiNO_3$	38.66	71.44	1.3358	1.336	14.2
5	NaF	50.11	55.4[a]	1.4008		14.7
6	$NaIO_3$	50.11	40.5	1.1928		13.2
7	NaH_2PO_4	50.11	39.99[b]	1.1843		13.1
8	$NaBrO_3$	50.11	55.8	1.4060		14.7
9	NaCl	50.11	76.35	1.6110	1.610	16.1
10	$NaNO_2$	50.11	57.79[b]	1.4294		14.9
11	$NaClO_3$	50.11	64.6	1.5028		15.4
12	NaBr	50.11	78.2	1.6263		16.2
13	$NaNO_3$	50.11	71.44	1.5683	1.568	15.8
14	$NaClO_4$	50.11	67.3	1.5296		15.5
15	NaI	50.11	76.8	1.6159		16.1
16	$NaCH_3CO_2$	50.11	40.9	1.1993		13.2
17	KF	73.52	55.4[a]	1.6828		16.6
18	KCl	73.52	76.35	1.9948	1.993	18.5
19	KBr	73.52	78.2	2.0182		18.7
20	$KClO_3$	73.52	64.6	1.8315		17.5
21	KNO_3	73.52	71.44	1.9297	1.886	18.1
22	$KClO_4$	73.52	67.3	1.8714		17.8
23	RbCl	77.8	76.35	2.0516		18.9
24	RbBr	77.8	78.2	2.0764		19.1
25	CsCl	77.3	76.35	2.0453		18.9
26	CsBr	77.3	78.2	2.0700		19.0
27	NH_4Cl	73.4	76.35	1.9933	1.994	18.5
28	$MgCl_2$	53.06	76.35	1.2502	1.249	13.6
29	$MgBr_2$	53.06	78.2	1.2625		13.7
30	$Mg(NO_3)_2$	53.06	71.44	1.2160	1.602	13.3
31	$CaCl_2$	59.50	76.35	1.3355	1.335	14.2
32	$SrCl_2$	59.46	76.35	1.3351		14.2
33	$BaCl_2$	63.64	76.35	1.3865	1.385	14.6

[a] From Robinson and Stokes.[30]
[b] By extrapolation using conductivity data in ref. 31.

branes[18] were used at the operating pressure of 250 psig. The specifications[13b] of membranes used are given in Table II in terms of pure water permeability constant A (in g-mole $H_2O/cm^2 \cdot sec \cdot atm$) and solute transport parameter ($D_{AM}/K\delta$) for sodium chloride (in cm/sec) at 250 psig. Table II also includes solute separation and product rate data for the membranes used at the operating pressure of 250 psig with 3500 ppm NaCl–H_2O feed solutions at feed flow rates corresponding to a mass transfer coefficient of 16.1×10^{-4} cm/sec on the high-pressure side of the membrane.

TABLE II
Film Specifications

Film no.	1	2	3	4	5	6	7
250 psig							
Pure-water permeability constant							
A, $\left(\frac{\text{g-mole } H_2O}{cm^2 \cdot sec \cdot atm}\right) \times 10^6$	1.61	2.06	3.40	5.56	1.76	2.38	3.83
Solute transport parameter							
$(D_{AM}/K\delta)_{NaCl}$, (cm/sec) $\times 10^5$	1.85	5.87	15.79	39.4	2.23	6.10	17.70
Solute separation, %	94.39	85.46	74.70	54.50	93.90	85.00	74.70
Product rate, g/hr[a]	18.89	24.74	40.0	63.0	20.59	28.64	45.0

[a] Area of film surface: 13.52 cm²; film pressurized at 300 psig; feed concentration: 3500 ppm NaCl–H_2O; mass transfer coefficient: 16.1×10^{-4} cm/sec.

In all experiments used for determining ionic parameters, the solute concentration in the feed solution was ~300 ppm so that the osmotic pressure of the feed solution was negligible compared to the operating pressure. Consequently, in each of these experiments, the product rate (PR) was practically the same as the pure water permeation rate (PWP). All experiments were of the short run type, and they were carried out at the laboratory temperature (23–25°). The (PR) and (PWP) data used in calculations were those corrected to 25°C using the relative viscosity and density data for pure water. The terms "product" and "product rate" refer to membrane-permeated solutions. The fraction solute separation f obtained in each experiment was calculated from the relation

$$f = \frac{\text{solute ppm in feed} - \text{solute ppm in product}}{\text{solute ppm in feed}}.$$

In each experiment, (PWP) and (PR) in grams per hour per given area of film surface (13.52 cm² in the apparatus used) and f were determined at the operating conditions employed. The concentration of solute in feed and product solutions were accurately determined in each case using a conductivity bridge.

RESULTS AND DISCUSSION

Born Equation for Ion–Solvent Interaction

The Born expression for the free energy (ΔG) of ion–solvent interaction is given as[15]

$$\Delta G = -N \frac{(Z_i e_0)^2}{2r_i}\left(1 - \frac{1}{\epsilon_s}\right) \tag{1}$$

where N = Avogadro number, Z_i = valence of the ion, e_0 = electronic charge, r_i = radius of the ion, and ϵ_s = dielectric constant of solvent. Let

$$E = N \frac{(Z_i e_0)^2}{2}\left(1 - \frac{1}{\epsilon_s}\right). \tag{2}$$

Then, eq. (1) can be written as

$$\Delta G = -\frac{E}{r_i}. \tag{3}$$

When ΔG is more negative, the ion is more stable in solution. Equation (1) predicts that the smaller the ion, the higher its valency, and/or the larger the dielectric constant of the solvent, the greater is the magnitude of the free energy change in the negative direction.

In Born's model, ions are represented as charged spheres, and the solvent is treated as a fluid of uniform dielectric constant. Since ions are not actually hard spheres, and the dielectric constant for the solvent in the vicinity of the ion should be different from that of ion-free solvent, eq. (3) can only be an approximate expression for ΔG. Data on hydration energies of monatomic ions show that ion–solvent interaction as expressed by Born equation is generally stronger than that shown by the experimental data.[15,16] Further, it has been shown[15,16,19,20] that by adjusting the values of the ionic radii in eq. (3) to differ from the crystallographic radii, one can obtain a good agreement between calculated and experimental values of ΔG for monatomic ions. Consequently, for practical applications involving ΔG, eq. (3) may be modified as

$$\Delta G = -\frac{E}{r_i + \Delta}. \tag{4}$$

Equation (4) can be rewritten as

$$\frac{1}{\Delta G} = -\frac{r_i + \Delta}{E} \tag{5}$$

$$= -\frac{1}{E} r_i - \frac{\Delta}{E}. \tag{6}$$

Equation (6) implies that the plot of $1/\Delta G$ versus r_i is a straight line whose slope and intercept represent $-1/E$ and $-\Delta/E$, respectively.

Using the data on free energy of hydration ΔG and the Pauling ionic radii listed in Table III (taken from ref. 20), the values of $1/\Delta G$ were plotted against r_i in Figure 1 for monovalent cations (plot A), divalent cations (plot B), and monovalent anions (plot C). The results showed that the data fell reasonably well on straight lines [confirming the validity of eq. (6)], and the slope and intercept for each straight-line plot were different for each class of ions. From the straight-line plots A, B, and C shown in Figure 1, the values of $-1/E$ and $-\Delta/E$, and hence the values of E and Δ, for each class of ions were calculated, and the results obtained are given in Table IV. Since these values of E and Δ refer to ions in bulk solution, they are designated as E_B and Δ_B, where the subscript B refers to bulk phase for which eq. (6) may be written as

$$\frac{1}{\Delta G_B} = -\frac{1}{E_B} r_i - \frac{\Delta_B}{E_B}. \tag{7}$$

Using the values of E_B and Δ_B obtained above for each class of ions (Table IV), the values of ΔG_B were back calculated for different ions using eq. (7). The results obtained are also given in Table III, which shows good agreement between the calculated and literature values of ΔG_B.

TABLE III
Free Energy Parameters for Some Monovalent and Divalent Ions

Ions	Ionic radius, Å	ΔG_B, kcal/mole: from ref. 20	ΔG_B, kcal/mole: from eq. (7)	ΔG_I, kcal/mole	$\Delta\Delta G$, kcal/mole	$\left(-\frac{\Delta\Delta G}{RT}\right)_i$
Monovalent cations						
Li^+	0.60	−123.5	−122.15	−125.57[a]	−3.42[a]	5.77[b]
Na^+	0.95	−98.3	−98.91	−102.34	−3.43	5.79
K^+	1.33	−80.8	−81.98	−85.48	−3.50	5.91
Rb^+	1.48	−76.6	−76.79	−80.26	−3.47	5.86
Cs^+	1.69	−71.0	−70.54	−73.93	−3.39	5.72
NH_4^+	—	—	—	—	−3.54	5.97
Divalent cations						
Mg^{++}	0.65	−455.5	−449.58	−452.38	−2.80	4.73
Ca^{++}	0.99	−380.8	−373.15	−376.24	−3.09	5.22
Sr^{++}	1.13	−345.9	−348.74	−351.85	−3.11	5.25
Ba^{++}	1.35	−315.5	−316.23	−319.33	−3.10	5.23
Monovalent anions						
F^-	1.36	−103.8	−103.88	−100.97	2.91	−4.91
IO_3^-	—	—	—	—	3.37	−5.69
$H_2PO_4^-$	—	—	—	—	3.65	−6.16
BrO_3^-	—	—	—	—	2.90	−4.89
Cl^-	1.81	−75.8	−74.84	−72.22	2.62	−4.42
NO_2^-	—	—	—	—	2.28	−3.85
ClO_3^-	—	—	—	—	2.43	−4.10
Br^-	1.95	−72.5	−68.86	−66.34	2.52	−4.25
NO_3^-	—	—	—	—	2.17	−3.66
ClO_4^-	—	—	—	—	2.13	−3.60
I^-	2.16	−61.4	−61.48	−59.12	2.36	−3.98
$CH_3CO_2^-$	—	—	—	—	2.90	−4.89

[a] Based on $(-\Delta\Delta G/RT)_i$.

[b] Obtained by using $\ln (D_{AM}/K\delta)_{LiCl}$, $\ln C^*$, and $\left(-\frac{\Delta\Delta G}{RT}\right)_{Cl^-}$.

TABLE IV
Values of E_B, Δ_B, E_I, and Δ_I for Monovalent Cations and Anions and Divalent Cations[a]

Plot	Class of ions	Slope $(-1/E_B) \times 10^3$	Intercept $(-\Delta/E_B) \times 10^3$	E_B	Δ_B	E_I	Δ_I
A	Monovalent cations	5.51	4.90	182.0	0.89	197.1	0.976
B	Divalent cations	1.34	1.35	746.3	1.01	760.0	1.03
C	Monovalent anions	8.30	−1.70	120.5	−0.20	114.1	−0.23

[a] E_B and E_I in kcal/mole; Δ_B and Δ_I in Å.

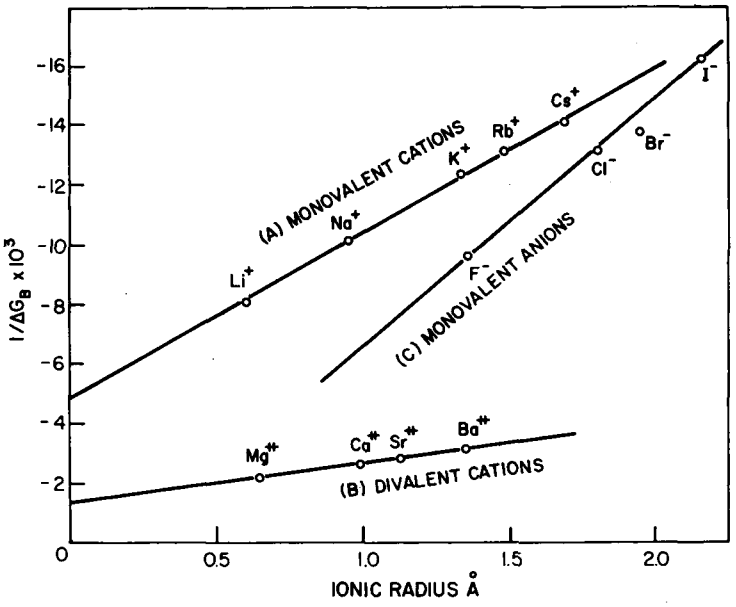

Fig. 1. Ionic radius vs. $1/\Delta G_B$ for monovalent cations, divalent cations, and monovalent anions.

Free Energy Requirement for Relative Repulsion or Attraction of Ions at the Membrane–Solution Interface

Since the ions are subject to electrostatic interaction in the vicinity of the membrane surface, the values of E_B and Δ_B obtained above for the bulk solution phase are not applicable for the membrane–solution interface. Assuming, however, that the form of eq. (6) is applicable for the interfacial region, eq. (6) can be rewritten as follows for ion–solvent interaction at the membrane–solution interface:

$$\frac{1}{\Delta G_I} = -\frac{1}{E_I} r_i - \frac{\Delta_I}{E_I} \tag{8}$$

where the subscript I refers to the interfacial region. Therefore, the energy needed to bring the ion from the bulk phase to the interface may be given as

$$\Delta\Delta G = \Delta G_I - \Delta G_B \tag{9}$$

$$= \left(-\frac{E_I}{r_i + \Delta_I}\right) - \left(-\frac{E_B}{r_i + \Delta_B}\right) \tag{10}$$

When $\Delta\Delta G$ is positive, it means that it requires energy to bring the ion from the bulk phase to the vicinity of the membrane surface, which in turn means that the ion is repelled by the material of the membrane surface. Similarly, when $\Delta\Delta G$ is negative, it means that the ion is more stable at the vicinity of the membrane surface which in turn means that the ion is

attracted by the material of the membrane surface. When $\Delta\Delta G$ is zero, it means that the ion is neither attracted nor repelled by the material of the membrane surface. At this point, it must be made clear that the quantity $\Delta\Delta G$ refers only to the interaction of the membrane material with the ion in aqueous solution, and the sign or the magnitude of $\Delta\Delta G$ says nothing about the preferential sorption characteristics of the membrane material for water itself. The following discussion is restricted to the case where water is preferentially sorbed at the membrane–solution interface.

Parameter Governing Reverse Osmosis Transport of Ions Through the Membrane

It is now useful to digress for a moment and recall Taft's discussion on the thermodynamic basis of the Hammett and Taft equations.[21] Using the notation of Taft,[21] the standard free energy change ($\Delta\Delta F^0$) representing the effect of structure on equilibria is given by the relation

$$\Delta\Delta F^0 = -RT \ln (K/K_0) \tag{11}$$

where K and K_0 represent the equilibrium constant for the reaction under consideration and a similar reaction taken as reference, respectively. The transition state theory of reaction rates leads to the result that relative rates are simply a special case of relative equilibria, i.e.,

$$(k/k_0) = (K^{\ddagger}/K_0{}^{\ddagger}) \tag{12}$$

where k and k_0 refer to the reaction rate constants and $K^{\ddagger}$ and $K_0{}^{\ddagger}$ refer to the corresponding equilibrium constants at the transition state. Consequently, the transition state free energy change ($\Delta\Delta F^{\ddagger}$) representing the effect of structure on reaction rate may be given as

$$\Delta\Delta F^{\ddagger} = -RT \ln (k/k_0). \tag{13}$$

The Hammett equation representing the effect of structure on reaction rate or equilibrium is given by the relation

$$\ln (k/k_0) = \sigma\rho \tag{14}$$

where σ is the Hammett number for the substituent group in the molecule and ρ is a proportionality constant characteristic of the functional group in the molecule and the reaction conditions involved. The analogous Taft equation corresponding to Hammett equation is given by

$$\ln (k/k_0) = \sigma^*\rho^* \tag{15}$$

where σ^* is the Taft number for the substituent group in the molecule, and ρ^* is a proportionality constant similar to ρ in eq. (14). From eqs. (13), (14), and (15),

$$(-\Delta\Delta F^{\ddagger}/RT) = \sigma\rho \text{ or } \sigma^*\rho^*. \tag{16}$$

It may also be recalled that the quantity on the right-hand side of eq. (16) has been used successfully to express the solute transport parameter in reverse osmosis for those solutes whose reverse osmosis transport is governed primarily by polar effects. For example, it has been shown[17] that for alcohols in limited ranges of σ^* or $\Sigma\sigma^*$,

$$(D_{AM}/K\delta) = C^* \exp(\rho^*\Sigma\sigma^*) \tag{17}$$

or

$$\ln (D_{AM}/K\delta) = \ln C^* + \rho^*\Sigma\sigma^* \tag{18}$$

where $(D_{AM}/K\delta)$ represents the solute transport parameter for alcohol, $\Sigma\sigma^*$ is the sum of the Taft numbers for the substituent groups in the alcohol, ρ^* is the applicable proportionality constant for the functional group —OH under the experimental conditions used, and C^* is another constant depending on the porous structure of the membrane surface.

One may now apply the basic concepts represented by eqs. (16) and (17) to the reverse osmosis transport of ionic solutes. Comparing eqs. (10) and (16), one may consider that the quantities $\Delta\Delta G$ and $\Delta\Delta F^{\pm}$ have similar thermodynamic basis, and hence the quantity $(-\Delta\Delta G/RT)$ is analogous to the quantity $\rho^*\Sigma\sigma^*$ in reverse osmosis transport. Thus the quantity $(-\Delta\Delta G/RT)$ emerges as a relevant parameter governing the reverse osmosis transport of ions through the membrane. Let this parameter be called the free energy parameter for ion for reverse osmosis transport, and let $(-\Delta\Delta G/RT)_i$ represent this parameter for each ion in solution. Following the form of eqs. (17) and (18), the solute transport parameter $(D_{AM}/K\delta)$ for the electrolytic solute as a whole may be expressed as

$$(D_{AM}/K\delta) = C^* \exp\{\Sigma(-\Delta\Delta G/RT)_i\} \tag{19}$$

so that

$$\ln (D_{AM}/K\delta) = \ln C^* + \Sigma(-\Delta\Delta G/RT)_i \tag{20}$$

where $\Sigma(-\Delta\Delta G/RT)_i$ represents the sum of the values of $(-\Delta\Delta G/RT)_i$ for each ion in the feed solution.

Equation (20) is significant. It shows that if the applicable values of $(-\Delta\Delta G/RT)_i$ for various cations and anions are known, they can be used to calculate $(D_{AM}/K\delta)$ values for each of the electrolytic solutes involving the above ions for any membrane for which ln C^* value is known; this latter value can be obtained from the $(D_{AM}/K\delta)$ data for any one electrolytic solute. Therefore, the problem is to obtain the numerical values of $(-\Delta\Delta G/RT)_i$ for various cations and anions applicable for reverse osmosis systems involving aqueous solutions and cellulose acetate membrane material. Such numerical values can be obtained from experimental reverse osmosis data for different electrolytic solutes. The procedure used to obtain such data, and the utility of these data for predicting solute separation involving different ions, are illustrated below.

Experimental Data on $(D_{AM}/K\delta)$ for Different Electrolytic Solutes

Using the experimental solute separation f and product rate (PR) data, the values of $(D_{AM}/K\delta)$ for each solute for the different films tested were calculated from the following expression applicable for dilute solutions:

$$(D_{AM}/K\delta) = \frac{(PR)}{3600\,Sd} \cdot \frac{1-f}{f}\left[\exp\frac{(PR)}{3600\,Skd}\right]^{-1} \tag{21}$$

where S = effective membrane area (= 13.52 cm²), k = mass transfer coefficient on the high-pressure side of the membrane (cm/sec), and d = density of solution (g/cm³). Equation (21) has been derived.[17] Again, as in previous work,[22] the values of k were obtained from the relation

$$k = k_{\text{ref}}\left[\frac{D_{AB}}{(D_{AB})_{\text{ref}}}\right]^{2/3} \tag{22}$$

where k_{ref} = mass transfer coefficient on the high-pressure side of the membrane for the reference solution system 3500 ppm NaCl–H_2O (= 16.1×10^{-4} cm/sec) and $(D_{AB})_{\text{ref}}$ and D_{AB} refer to diffusivity of sodium chloride and the salt under consideration, respectively, in water. The values of D_{AB} (in cm²/sec) of the various electrolytic solutes in very dilute aqueous solutions were obtained from the Nernst equation[23]

$$D_{AB} = \frac{(1/Z_+ + 1/Z_-)RT}{(1/\lambda_+^0 + 1/\lambda_-^0)F_a^2} \tag{23}$$

where Z_+ and Z_- are the valencies of cation and anion, respectively; R = gas constant = 8.316 joules/(°K)(g-mole); T = absolute temperature, °K; λ_+^0 and λ_-^0 = limiting (zero concentration) ionic conductances, amp/(cm²)(volt/cm)(g-equivalent/cm³); and F_a = Faraday = 96500 coulombs/g-equivalent. For all solutes studied in this work, the values of λ_+^0, λ_-^0, and D_{AB} calculated from eq. (23) and the values of k calculated from eq. (22) are given in Table I.

Numerical Values for the Free Energy Parameter for Ions

The numerical values of the free energy parameter developed above are independent of the porous structure of the membrane. For the purpose of calculating these values, the reverse osmosis data (i.e., $(D_{AM}/K\delta)$ data) obtained for different solutes with the same film (whose surface pore structure remained constant in all experiments) should be used; the data obtained with film 2 were arbitrarily chosen for illustrating the calculation procedure.

Monatomic Monovalent Cations. Consider the $(D_{AM}/K\delta)$ values obtained with film 2 for LiCl, NaCl, KCl, RbCl, and CsCl. With reference to $(D_{AM}/K\delta)$ data for the pair of solutes LiCl and KCl, eq. (20) can be written as

$$\ln (D_{AM}/K\delta)_{\text{LiCl}} = \ln C^* + \left\{\left(-\frac{\Delta\Delta G}{RT}\right)_{\text{Li}^+} + \left(-\frac{\Delta\Delta G}{RT}\right)_{\text{Cl}^-}\right\} \tag{24}$$

$$\ln (D_{AM}/K\delta)_{KCl} = \ln C^* + \left\{\left(-\frac{\Delta\Delta G}{RT}\right)_{K^+} + \left(-\frac{\Delta\Delta G}{RT}\right)_{Cl^-}\right\}. \quad (25)$$

The quantity $\ln C^*$ is a measure of the porous structure of the membrane surface, and its value is assumed identical in eqs. (24) and (25) since the $(D_{AM}/K\delta)$ data refer to the same film. This assumption is verified later (Table V). Subtracting eq. (25) from eq. (24), and using eq. (10),

$$\ln (D_{AM}/K\delta)_{LiCl} - \ln (D_{AM}/K\delta)_{KCl} = \left(-\frac{\Delta\Delta G}{RT}\right)_{Li^+} - \left(-\frac{\Delta\Delta G}{RT}\right)_{K^+} \quad (26)$$

$$= \frac{1}{RT}\left\{\left(\frac{E_I}{r_{Li^+} + \Delta_I} - \frac{E_B}{r_{Li^+} + \Delta_B}\right) - \left(\frac{E_I}{r_{K^+} + \Delta_I} - \frac{E_B}{r_{K^+} + \Delta_B}\right)\right\} \quad (27)$$

$$= \frac{1}{RT}\left\{\left(\frac{E_I}{r_{Li^+} + \Delta_I} - \frac{E_I}{r_{K^+} + \Delta_I}\right) - \left(\frac{E_B}{r_{Li^+} + \Delta_B} - \frac{E_B}{r_{K^+} + \Delta_B}\right)\right\}. \quad (28)$$

Rearranging eq. (28),

$$E_I \cdot \frac{(r_{Li^+} - r_{K^+})}{(r_{Li^+} + \Delta_I)(r_{K^+} + \Delta_I)} = -RT\{\ln (D_{AM}/K\delta)_{LiCl} - \ln (D_{AM}/K\delta)_{KCl}\} + E_B \cdot \frac{(r_{Li^+} - r_{K^+})}{(r_{Li^+} + \Delta_B)(r_{K^+} + \Delta_B)} \quad (29)$$

The right side of eq. (29) can now be evaluated since the numerical value of each one of the quantities involved (namely, $\ln (D_{AM}/K\delta)_{LiCl}$, $\ln (D_{AM}/K\delta)_{KCl}$, E_B, Δ_B, r_{Li^+}, and r_{K^+}) is known. Let K_{Li^+,K^+} represent the right side of eq. (29) so that

$$E_I \cdot \frac{(r_{Li^+} - r_{K^+})}{(r_{Li^+} + \Delta_I)(r_{K^+} + \Delta_I)} = K_{Li^+,K^+}. \quad (30)$$

Similar calculations can be made with reference to $(D_{AM}/K\delta)$ data for the pairs of solutes NaCl and KCl, RbCl and KCl, and CsCl and KCl, so that the following equations, analogous to eq. (30), can be written:

$$E_I \cdot \frac{(r_{Na^+} - r_{K^+})}{(r_{Na^+} + \Delta_I)(r_{K^+} + \Delta_I)} = K_{Na^+,K^+} \quad (31)$$

$$E_I \cdot \frac{r_{Rb^+} - r_{K^+}}{(r_{Rb^+} + \Delta_I)(r_{K^+} + \Delta_I)} = K_{Rb^+,K^+} \quad (32)$$

$$E_I \cdot \frac{(r_{Cs^+} - r_{K^+})}{(r_{Cs^+} + \Delta_I)(r_{K^+} + \Delta_I)} = K_{Cs^+,K^+}. \quad (33)$$

The quantities K_{Na^+,K^+}, K_{Rb^+,K^+}, and K_{Cs^+,K^+} can be calculated from expressions analogous to the right side of eq. (29), using the appropriate

TABLE V
Experimental ln C^* Values

Solute	ln C^*
Films 2	
NaF	−11.11
NaCl	−11.11
NaBr	−11.13
NaI	−11.08
Film 6	
LiCl	−11.17
LiBr	−11.06
$LiNO_3$	−11.24
NaCl	−11.07
KF	−11.04
KCl	−11.02
KBr	−11.05
$KClO_3$	−10.90
KNO_3	−10.88
$KClO_4$	−10.92
RbCl	−11.18
RbBr	−11.08
CsCl	−11.12
CsBr	−11.16
$MgCl_2$	−10.80
$Mg(NO_3)_2$	−11.01
$CaCl_2$	−11.08
$SrCl_2$	−10.99
$BaCl_2$	−11.04

Film no.	ln C^* based on NaCl data
1	−12.27
3	−10.19
4	−9.37
5	−12.08
7	−10.09

numerical values of ln $(D_{AM}/K\delta)$ and r_t; the numerical values of E_B and Δ_B are the same (Table IV) for all the monovalent cations considered.

Dividing eq. (30) by eq. (31) and rearranging, one obtains

$$\frac{(r_{Na^+} + \Delta_I)}{(r_{Li^+} + \Delta_I)} - \frac{K_{Li^+,K^+}}{K_{Na^+,K^+}} \cdot \frac{(r_{Na^+} - r_{K^+})}{(r_{Li^+} - r_{K^+})} = 0. \tag{34}$$

Treating eqs. (30), (32), and (33) in a similar manner, one can obtain

$$\frac{(r_{Rb^+} + \Delta_I)}{(r_{Li^+} + \Delta_I)} - \frac{K_{Li^+,K^+}}{K_{Rb^+,K^+}} \cdot \frac{(r_{Rb^+} - r_{K^+})}{(r_{Li^+} - r_{K^+})} = 0 \tag{35}$$

$$\frac{(r_{Cs^+} + \Delta_I)}{(r_{Li^+} + \Delta_I)} - \frac{K_{Li^+,K^+}}{K_{Cs^+,K^+}} \cdot \frac{(r_{Cs^+} - r_{K^+})}{(r_{Li^+} - r_{K^+})} = 0. \tag{36}$$

A value of Δ_I can be obtained by solving any one of the eqs. (34), (35), or (36). The three values of Δ_I so obtained can be expected to be slightly different from each other in view of the different experimental data used in calculating the quantity on the right side of eq. (29) or its analogous expression. A value of Δ_I for practical use can be obtained by taking the average of the three Δ_I values obtained above. Such an average value for Δ_I was found to be 0.976 Å. Using this value of Δ_I, one can calculate the value of E_I from each of the eqs. (30), (31), (32), and (33); the values of E_I (in kcal/mole) so obtained were 197.87, 195.15, 198.82, and 196.63, respectively, yielding an average value of 197.11 for E_I. Therefore, for practical purposes, the values of E_I and Δ_I for monovalent cations can be taken to be 197.1 kcal/mole and 0.976 Å, respectively. Since the values of E_B and Δ_B for monovalent cations are already known (Table IV), eq. (10) can be written as

$$\Delta\Delta G = \left(-\frac{197.1}{r_i + 0.976}\right) - \left(-\frac{182.0}{r_i + 0.89}\right) \tag{37}$$

and the parameter $(-\Delta\Delta G/RT)_i$ for reverse osmosis transport of monovalent cations through cellulose acetate membranes can be given as

$$\left(-\frac{\Delta\Delta G}{RT}\right)_i = \frac{1}{0.5925}\left\{\left(\frac{197.1}{r_i + 0.976}\right) - \left(\frac{182.0}{r_i + 0.89}\right)\right\}. \tag{38}$$

The values of $(-\Delta\Delta G/RT)_i$ calculated from eq. (38) for the monovalent cations Li^+, Na^+, K^+, Rb^+, and Cs^+ are given in Table III.

Monatomic Divalent Cations. The values of $(-\Delta\Delta G/RT)_i$ for divalent cations can be obtained by the same technique described above for monovalent cations. Using the ln $(D_{AM}/K\delta)$ data obtained with film 2 for $MgCl_2$, $CaCl_2$, $SrCl_2$, and $BaCl_2$, the values of Δ_I and E_I were calculated to be 1.03 Å, and 760.0 kcal/mole, respectively. Therefore the parameter $(-\Delta\Delta G/RT)_i$ for reverse osmosis transport of divalent cations through cellulose acetate membranes can be given as:

$$\left(-\frac{\Delta\Delta G}{RT}\right)_i = \frac{1}{0.5925}\left\{\left(\frac{760.0}{r_i + 1.03}\right) - \left(\frac{746.3}{r_i + 1.01}\right)\right\}. \tag{39}$$

The values of $(-\Delta\Delta G/RT)_i$ calculated from eq. (39) for the divalent cations Mg^{++}, Ca^{++}, Sr^{++}, and Ba^{++} are given in Table III.

Monatomic Monovalent Anions. The values of $(-\Delta\Delta G/RT)_i$ for monovalent anions also can be obtained by the same technique described above for monovalent cations. For this purpose, the salts chosen must have the same cation. Using the ln $(D_{AM}/K\delta)$ data obtained with film 2 for NaF, NaCl, NaBr, and NaI, the values of Δ_I and E_I were calculated to be -0.23 Å and 114.1 kcal/mole, respectively. Therefore, the parameter $(-\Delta\Delta G/RT)_i$ for reverse osmosis transport of monovalent anions through cellulose acetate membranes can be given as

$$\left(-\frac{\Delta\Delta G}{RT}\right)_i = \frac{1}{0.5925}\left\{\left(\frac{114.1}{r_i - 0.23}\right) - \left(\frac{120.5}{r_i - 0.20}\right)\right\}. \tag{40}$$

The values of $(-\Delta\Delta G/RT)_i$ calculated from eq. (40) for the monovalent anions F^-, Cl^-, Br^-, and I^- are given in Table III.

Polyatomic Monovalent Cations and Anions. This work also included studies on solutes involving the following polyatomic ions: NH_4^+, IO_3^-, $H_2PO_4^-$, BrO_3^-, NO_2^-, ClO_3^-, NO_3^-, ClO_4^-, and CH_3COO^-. While crystallographic data on ionic radii for monatomic ions seem firmly established in the literature, the meaning of similar data for polyatomic ions, especially those capable of hydrogen bonding, is probably subject to significant uncertainty. For this reason, the values of $(-\Delta\Delta G/RT)_i$ for the above polyatomic ions were determined directly from eq. (20) using the known values of the ionic parameters for monatomic ions and experimental $(D_{AM}/K\delta)$ data. For example, with reference to film 2, using the experimental $(D_{AM}/K\delta)$ data for NaCl, and the values of $(-\Delta\Delta G/RT)_i$ obtained above for Na^+ and Cl^- ions, the value of ln C^* for the film was first calculated using eq. (20). Then using the experimental $(D_{AM}/K\delta)$ data for NH_4Cl and the known values of ln C^* and $(-\Delta\Delta G/RT)_i$ for Cl^- ion, the value of $(-\Delta\Delta G/RT)_i$ for NH_4^+ ion was calculated again from eq. (20). Similarly, the value of $(-\Delta\Delta G/RT)_i$ for the polyatomic anions listed above were calculated using the known values of ln C^* for the film and $(-\Delta\Delta G/RT)_i$ for Na^+ ion, and the experimental $(D_{AM}/K\delta)$ values of the corresponding sodium salts involving each of the anions. The values of $(-\Delta\Delta G/RT)_i$ so obtained for the polyatomic ions listed above are given in Table III.

Ionic Parameter for Li^+ Ion. The value of $(-\Delta\Delta G/RT)_i$ for Li^+ ion calculated from eq. (38) was 4.93, whereas that calculated directly from eq. (20) (using the experimental $(D_{AM}/K\delta)$ data for LiCl and NaCl and the known ionic parameters for Na^+ and Cl^- ions) was 5.77. The latter value is taken as the appropriate value for the ionic parameter of Li^+ ion, since it was found to be consistent with the experimental reverse osmosis data obtained for LiCl and other lithium salts with several membranes. The values of ΔG_I and $\Delta\Delta G$ for Li^+ listed in Table III were obtained using the latter value of $(-\Delta\Delta G/RT)_i$ for Li^+.

Correlations of Lyotropic Number with ΔG_B, ΔG_I, and $\Delta\Delta G$. The correspondence between the order of solute separation in reverse osmosis and the order of the lyotropic series of ions,[24] as well as some exceptions to this correspondence in order, have been pointed out.[13,25] The reason for the existence, and the lack of existence, of the above correspondence in order becomes explicit from Figure 2 which gives the correlations between lyotropic number[24] and ΔG_B, ΔG_I, and $\Delta\Delta G$ of different ions. Figure 2 shows the existence of unique relationships (not necessarily linear) between lyotropic number and the quantities ΔG_B and ΔG_I with respect to the cations Li^+, Na^+, K^+, Rb^+, and Cs^+, and the anions F^-, Cl^-, Br^-, and I^-. However, the controlling parameter for reverse osmosis separation is $\Delta\Delta G$, which is the difference between the quantities ΔG_I and ΔG_B. The correlation between $\Delta\Delta G$ and lyotropic number shows that with respect to the halide anions, $\Delta\Delta G$ decreases with increase in lyotropic number; this order

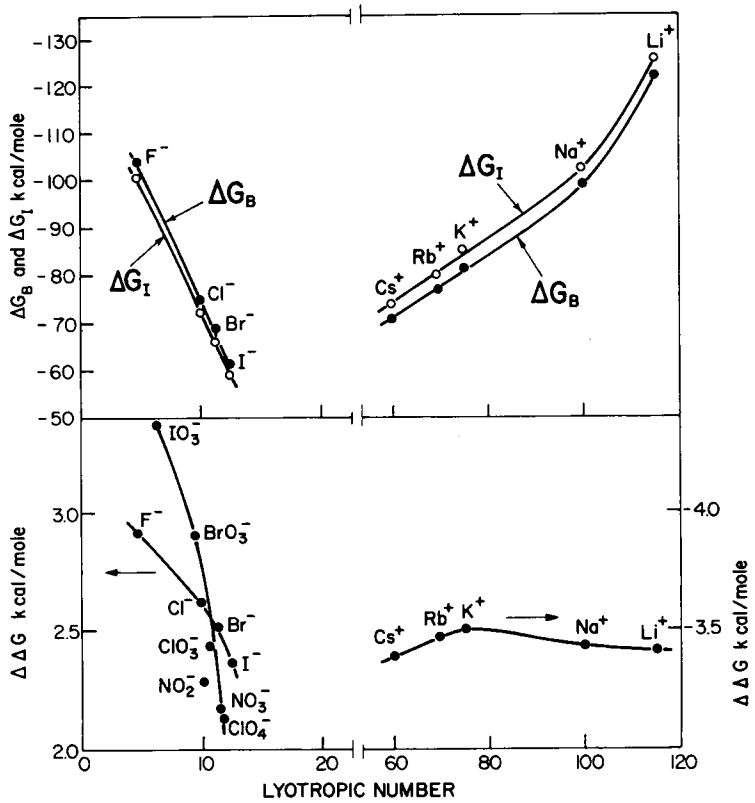

Fig. 2. Lyotropic number *vs.* ΔG_B, ΔG_I, and $\Delta\Delta G$ for monovalent cations and anions.

is seen in reverse osmosis separation also (Tables VI and VII). With respect to the alkali metal cations, $\Delta\Delta G$ passes through a slight minimum for K^+ with increase in lyotropic number. This order seems consistent with the experimental reverse osmosis separation data given in Table VII, even though differences in separations among lithium, sodium, and potassium salts for the membranes tested are practically insignificant. Further, it may be noted that the form of the lyotropic number-versus-$\Delta\Delta G$ correlation for alkali metal cations is exactly similar to the selectivity sequence given for these ions by Krasne and Eisenman (see their Fig. 50 in ref. 5).

The $\Delta\Delta G$-versus-lyotropic number correlation for polyatomic anions capable of hydrogen bonding is different from that for halide anions as seen in Figure 2. The data show that $\Delta\Delta G$ decreases steeply with increase in lyotropic number for the polyatomic anions considered. Their reverse osmosis separations also decrease steeply with increase in lyotropic number as shown by the data given in Table VI.

It must, however, be pointed out that the numerical values of $\Delta\Delta G$ for the different ions and their correlation with lyotropic numbers can change with change in the chemical nature of the membrane material, solvent, and/

TABLE VI
Comparison of Calculated and Experimental Reverse Osmosis Separations for Some Sodium Salts and Ammonium Chloride[c]

Solute no.	Solute	Solute separation, %							
		Film 1		Film 2		Film 3		Film 4	
		Calcd.	Exptl.	Calcd.	Exptl.	Calcd.	Exptl.	Calcd.	Exptl.
5	NaF	96.9	95.7	91.9	91.9	85.0	85.8	72.9	74.7
6	$NaIO_3$	98.5	98.4	a	96.0	92.0	94.9		b
7	NaH_2PO_4	99.1	99.3	a	97.4	94.7	96.1	88.8	90.7
8	$NaBrO_3$	96.9	97.2	a	91.9	84.8	85.6	71.7	71.7
9	NaCl	a	95.2	a	88.0	a	78.7	a	63.7
10	$NaNO_2$	91.7	89.9	a	80.2	66.6	68.4	47.6	48.3
11	$NaClO_3$	93.5	92.7	a	84.2	72.4	73.2	54.8	54.3
12	NaBr	94.4	94.4	86.2	86.5	75.9	78.2	59.9	58.9
13	$NaNO_3$	90.3	89.0	a	77.5	63.3	62.6	44.6	42.5
14	$NaClO_4$	89.7	87.3	a	76.2	61.5	62.1	42.7	41.6
15	NaI	92.8	91.9	82.6	82.2	70.6	70.2	52.7	50.6
16	CH_3COONa	96.1	94.2	a	91.6		b		b
27	NH_4Cl	94.5	94.9	a	86.5	77.0	75.6		b

[a] Experimental data used for calculating $(-\Delta\Delta G/RT)_i$ for the anion or ln C^*.
[b] Not determined.
[c] All the above data are for films specified in Table II, operating pressure of 250 psig, and k values given in Table I.

or reverse osmosis operating conditions of pressure and temperature. Consequently, one cannot expect an invarient order of solute separation in reverse osmosis with respect to different ions. Lyotropic series is caused by differences in ionic field strength, and hence lyotropic number is a fundamental physicochemical parameter for the ion expressing its relative tendency for electron transfer. Since this tendency is also a basis for reverse osmosis separations, it is reasonable to expect that whatever correlation exists between $\Delta\Delta G$ and lyotropic number, that will be reflected in the correlation between the latter and $(D_{AM}/K\delta)$ for the ionic solutes, and hence their separations, in reverse osmosis.

Sign and Magnitude of Ionic Parameters. Table III shows that the quantity $(-\Delta\Delta G/RT)_i$ is positive for all cations and negative for all anions. This shows that the cation is attracted and anion is repelled by the membrane surface which means that the membrane surface behaves as if it is negatively charged. This result confirms the observation made earlier[27] that the cellulose acetate material has a net proton acceptor character with respect to solute–membrane interactions.

The values of the ionic parameter for divalent cations are lower than those for the monovalent cations. This accounts for the relatively lower values for ln $(D_{AM}/K\delta)$ and hence higher values for solute separations with respect to solutes involving divalent cations. Also, Table III shows that the values of $(-\Delta\Delta G/RT)_i$ for halide anions increase with increase in ionic radius. This means that with respect to solutes involving halide

TABLE VII
Comparison of Calculated and Experimental Reverse Osmosis Separations for Different Salts[c]

Solute no.	Solute	Solute separation, %					
		Film 5		Film 6		Film 7	
		Calcd.	Exptl.	Calcd.	Exptl.	Calcd.	Exptl.
1	LiF	96.6	98.5		b		b
2	LiCl	94.3	94.2	87.7	87.4	76.2	76.0
3	LiBr	93.3	93.2	85.8	84.0	72.4	70.5
4	$LiNO_3$	88.6	88.9	77.2	77.9	60.9	62.7
9	NaCl	a	94.4	a	88.2	a	77.5
17	KF	96.2	94.8	91.8	91.5	84.6	86.1
18	KCl	94.1	94.5	87.8	87.2	77.3	76.4
19	KBr	92.9	93.7	85.6	85.3	74.0	73.6
20	$KClO_3$	91.9	91.2	83.0	81.1	69.8	67.9
21	KNO_3	88.1	86.5	75.2	73.3	61.0	58.9
22	$KClO_4$	87.4	86.3	74.7	72.7	59.3	57.7
23	RbCl	94.2	94.7	88.0	89.2	77.9	79.9
24	RbBr	93.4	94.5	86.5	86.7	75.4	75.8
25	CsCl	95.0	95.0	89.6	90.0	80.4	82.3
26	CsBr	94.2	94.5	87.9	87.5	77.7	77.5
28	$MgCl_2$	97.9	98.0	95.3	93.9	89.8	87.3
29	$MgBr_2$	97.5	96.9		b		b
30	$Mg(NO_3)_2$	95.6	96.1	90.3	89.8	80.2	80.3
31	$CaCl_2$	96.5	96.4	92.4	92.5	84.7	85.3
32	$SrCl_2$	96.4	95.8	92.2	91.7	84.2	84.6
33	$BaCl_2$	96.6	96.3	92.6	92.4	84.8	84.1

[a] Experimental data used to calculate ln C^*.
[b] Not determined.
[c] All the above data are for films specified in Table II, operating pressure of 250 psig, and k values given in Table I.

anions, ln $(D_{AM}/K\delta)$ increases, and hence solute separation decreases, with increase in ionic radius. A similar conclusion seems valid with respect to other anions as well.

The data also show that the values of the ionic parameter for the monovalent and divalent cations follow the sequence

$$Li^+ < Na^+ < K^+ > Rb^+ > Cs^+$$

and

$$Mg^{++} < Ca^{++} < Sr^{++} > Ba^{++}.$$

The above sequence is the same as that given by Choi and Bennion[8] based on relative ionic mobilities.

Table III also shows that the values of the ionic parameter for IO_3^-, BrO_3^-, and ClO_3^- are in the following order in the negative direction:

$$IO_3^- > BrO_3^- > ClO_3^-$$

which order is identical to the order of hydrogen bonding ability (basicity) of the ions in view of the electronegativity values of 2.5, 2.8, and 3.0 for I,

Br, and Cl, respectively.[28] The above order in the values of ionic parameter also confirms that the cellulose acetate membrane surface has a net basic character.

Utility of Data on Free Energy Parameter for Ions—An Illustration

The data on free energy parameter for ions given in Table III, together with eqs. (20) and (21), offer a means of predicting solute separation for various ionic solutes in aqueous solution from reverse osmosis data for the separation of any one reference solute only. The procedure for such prediction is as follows. Consider very dilute feed solutions and let NaCl be the reference solute. For any given film, first determine $(D_{AM}/K\delta)$ for NaCl from the experimental reverse osmosis data using eq. (21). Use this $(D_{AM}/K\delta)_{NaCl}$ to calculate ln C^* for the film from eq. (20). Then, for any desired solute, calculate ln $(D_{AM}/K\delta)$ from eq. (20) using the ln C^* value obtained above and the appropriate values of the ionic parameter taken from Table III. Finally, calculate solute separation for the desired solute from eq. (21) using the $(D_{AM}/K\delta)$ value for the solute calculated above and the required value of k. The values of (PR) and d may be assumed to be the same as those applicable for the reference system for very dilute feed solutions.

The use of a constant value for ln C^* in the above prediction procedure is justified on the basis of experimental data presented in Table V for films 2 and 6 chosen for illustration; the data for the other films tested were similar. The experimental results showed that, for a given film, the numerical value of ln C^* was essentially the same for each one of the electrolytic solutes used in the reverse osmosis experiments.

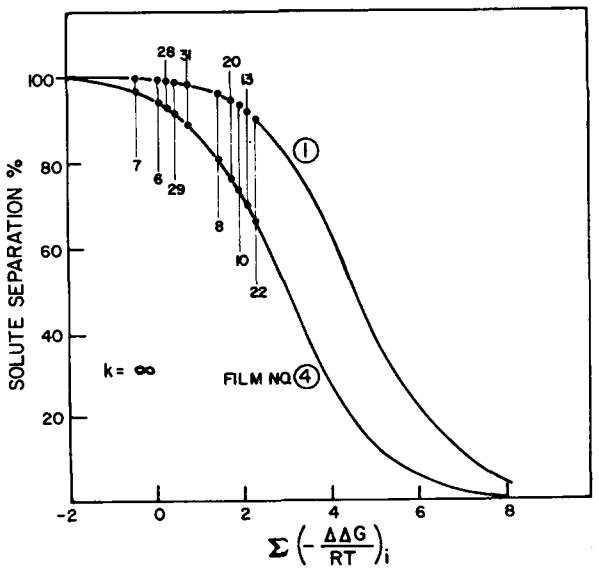

Fig. 3. Solute separation vs. $\Sigma(-\Delta\Delta G/RT)_i$ for $k = \infty$ at 250 psig. Solute numbers same as in Table I.

Using the ln C^* values (given in Table V) obtained from sodium chloride data only, solute separations were calculated for 32 other solutes using seven different films (films 1 to 7) following the procedure described above. The k values listed in Table I were used in these calculations. The calculated results were then compared with solute separation data actually obtained in the reverse ormosis experiments. The results, given in Tables VI and VII, showed excellent agreement between calculated and experimental values. The data involved in the above comparison of results cover a wide range of solute separations (42% to 98%); consequently, the concept of ionic parameters, and the prediction procedure illustrated above, have firm experimental basis and practical validity.

Referring to eq. (20), it is clear that, for a given membrane, $(D_{AM}/K\delta)$ is a function of the sum of the ionic parameters. Since it is conceivable to obtain the same sum by different combinations of ions, the correlation of $(D_{AM}/K\delta)$ versus $\Sigma(-\Delta\Delta G/RT)_i$ has a more fundamental significance. Further, since data on solute separation are of more practical interest and they are related to $(D_{AM}/K\delta)$ by eq. (21), a correlation of solute separation at $k = \infty$ versus $\Sigma(-\Delta\Delta G/RT)_i$ for various values of ln C^* can be useful. Such a correlation is illustrated in Figure 3 for films 1 and 4 for various assumed values of $\Sigma(-\Delta\Delta G/RT)_i$. These data were calculated by using the following form of eq. (21) applicable for the condition $k = \infty$:

$$f = \frac{1}{1 + (C^*/v_s) \exp\left\{\Sigma(-\Delta\Delta G/RT)_i\right\}} \tag{41}$$

where $v_s = (PR)/3600Sd$. The data corresponding to some of the solutes used in this work are also indicated in the correlations shown in Figure 3. It may be noted that the sum of the ionic parameters for the solutes used in this work lies only in a narrow range. However, the form of the correlations is exactly the same as those illustrated earlier[17] for alcohols. Figure 3 indicates the possibility of developing a unified scale of $(\Delta\Delta G/RT)$ parameter for both ionic and nonionic solutes for use in reverse osmosis transport equations.

CONCLUSIONS

The concept of the free energy parameter for reverse osmosis transport developed in this paper has firm theoretical and experimental foundation. The predictive capability of this parameter has been illustrated. Much further work is needed to explore the fullest potentialities of this concept in the further development of reverse osmosis. In particular, determination of the values of the above parameter for other ions and detailed work on the effect of pressure, temperature, feed concentration, and the chemical nature of the membrane on the values of $(-\Delta\Delta G/RT)_i$ and the utility of the parameter for predicting reverse osmosis separations in mixed solute systems are the areas of study which are of immediate interest.

The authors are grateful to R. Ironside for help and advice on analytical techniques.
Issued as N.R.C. No. 14402.

References

1. H. K. Lonsdale, U. Merten, and R. L. Riley, *J. Appl. Polym. Sci.*, **9**, 1341 (1965).
2. J. E. Anderson and M. E. Heyde, *Bull. Amer. Phys. Soc.*, **18**(3), 320 (1973).
3. G. Eisenman, *Biophys. J.*, **2**, 259 (1962).
4. J. M. Diamond and E. M. Wright, in *Annual Review of Physiology*, V. E. Hall, Ed., Annual Review Inc., Palo Alto, Calif., 1969, p. 581.
5. S. Krasne and G. Eisenman, in *Membranes*, Vol. 2, G. Eisenman, Ed., Marcel Dekker, New York, 1973, p. 277.
6. B. M. Misra and J. W. McCutchan, School of Engineering and Applied Science, University of California, Los Angeles, Report No. UCLA-ENG-7137, 1971.
7. G. Kamizawa and J. W. McCutchan, School of Engineering and Applied Science, University of California, Los Angeles, Report No. UCLA-ENG-7158, 1971.
8. K. W. Choi and D. N. Bennion, School of Engineering and Applied Science, University of California, Los Angeles, Report No. UCLA-ENG-7350, 1973.
9. Yu. N. Dytnerskii, G. V. Polyakov, and L. S. Lukavyi, *Teoreticheskie Osnovy Khimicheskoi Tekhnologii*, **6** (4), 628 (1972).
10. E. Glueckauf, in *Proceedings of the First International Symposium on Water Desalination*, Oct. 3–9, 1965, Vol. 1, Office of Saline Water, U.S. Department of the Interior, Washington, D.C., 1967, pp. 143–156.
11. E. Glueckauf and D. C. Sammon, in *Proceedings of Third International Symposium on Fresh Water from the Sea*, Dubrovnik, 13–17 September 1970, Vol. 2, pp. 397–422.
12. C. P. Bean, Research and Development Progress Report No. 465, Office of Saline Water, U.S. Department of the Interior, Washington, D.C., 1969.
13(a) S. Sourirajan, *Reverse Osmosis*, Academic Press, New York, 1970, Chap. 1; (b) *ibid.*, Chap. 3; (c) *ibid.*, Appendix II.
14. T. Matsuura and S. Sourirajan, *J. Appl. Polym. Sci.*, **15**, 2905 (1971).
15. J. O'M. Bockris and A. K. N. Reddy, *Modern Electrochemistry*, Vol. 1, Plenum, New York, 1970, Chap. 2.
16. C. S. G. Phillips and R. J. P. Williams, *Inorganic Chemistry*, Vol. 1, Oxford University Press, New York, 1965, p. 159.
17. T. Matsuura and S. Sourirajan, *J. Appl. Polym. Sci.*, **17**, 1043 (1973).
18. L. Pageau and S. Sourirajan, *J. Appl. Polym. Sci.*, **16**, 3185 (1972).
19. W. M. Latimer, K. S. Pitzer, and C. M. Slansky, *J. Chem. Phys.*, **7**, 108 (1939).
20. H. L. Friedman and C. V. Krishnan, in *Water—A Comprehensive Treatise*, F. Franks, Ed., Plenum, New York, 1973, Chap. 1.
21. R. W. Taft, Jr., in *Steric Effects in Organic Chemistry*, M. S. Newman, Ed., Wiley, New York, 1956, pp. 556–675.
22. T. Matsuura, M. E. Bednas, and S. Sourirajan, *J. Appl. Polym. Sci.*, **18**, 567 (1974).
23. R. C. Reid and T. K. Sherwood, *The Properties of Gases and Liquids*, McGraw-Hill, New York, 1958, p. 293.
24. A. Voet, *Chem. Rev.*, **20**, 169 (1937).
25. S. Sourirajan, *Ind. Eng. Chem.*, Fundam., **2**, 51 (1963).
26. D. F. C. Morris, *J. Inorg. Nucl. Chem.*, **6**, 295 (1958).
27. T. Matsuura and S. Sourirajan, *J. Appl. Polym. Sci.*, **16**, 1663 (1972).
28. L. Pauling, *The Nature of the Chemical Bond*, 2nd ed., Cornell University Press, Ithaca, N.Y., 1948, p. 60.
29. H. S. Harned and B. B. Owen, *The Physical Chemistry of Electrolytic Solutions*, 3rd ed., Reinhold, New York, 1958, p. 231.
30. R. A. Robinson and R. H. Stokes, *Electrolyte Solutions*, 2nd ed., Butterworths, London, 1959, pp. 461 and 463.
31. *Gmelins Handbuch der Anorganischen Chemie*, 8th ed., Natrium, Ergänzunsband Lieferung 4, System Nummer 21, Verlag Chemie GMBH, Weinheim, 1967, p. 1608.

Received June 12, 1974